

Impact on the estimated dose of different tissue assignment strategies during partial breast irradiations with INTRABEAM

P. Ibáñez^{1,2*}, A. Villa-Abaunza¹ and J.M. Udías^{1,2}

¹Nuclear Physics Group and IPARCOS, Department of Structure of Matter, Thermal Physics and Electronics, CEI Moncloa, Universidad Complutense de Madrid, Madrid, Spain

² Instituto de Investigación Sanitaria del Hospital Clínico San Carlos, Madrid, Spain

[*pbibanez@ucm.es](mailto:pbibanez@ucm.es)

Abstract

Partial breast irradiations with kilovoltage intraoperative radiation therapy devices such as INTRABEAM are becoming more common every day, because of the ease of use and the smaller cost compared to equivalent megavoltage treatments. Dose planning with INTRABEAM is usually based on water models. However, breast tissue is mainly composed of glandular and adipose tissues. While variations in the estimated dose in the different soft tissues are not significant in the case of conventional megavoltage photons, for X-rays this is not necessarily the case due to the dominance of photoelectric effect. Furthermore, adipose and glandular tissues are not always clearly disentangled in planning breast CTs. The aim of this work was to study the effect on the dose prescribed in breast with the INTRABEAM device with different soft tissue assignment strategies.

Dose was computed with a Monte Carlo code in five patients with a 3 cm diameter INTRABEAM spherical applicator. Tissues within the breast were assigned following six different strategies: one based on the TG-43 recommendations, representing the whole breast as water of unity density, another one also water-based but with CT derived density, and the other four also based on CT-derived densities, using a single tissue resulting from different mixes of glandular and adipose tissues. These were compared against the reference dose computed in an accurately segmented CT, following TG-186 recommendations. Relative differences and dose ratios between the reference and the other tissue assignment strategies were obtained in three regions of interest inside the breast. Dose planning in water-based tissues was found inaccurate for breast treatment with INTRABEAM, as it would incur in up to 30% under-prescription of dose. If accurate soft tissue assignments in the breast cannot be safely done, a single-tissue composition of 80% adipose and 20% glandular tissue, or even a 100% adipose tissue, avoids under-prescribing dose.

Keywords: low-energy X-ray IORT, Monte Carlo, partial breast irradiation, breast tissue composition, dose calculation

1. INTRODUCTION

Traditionally, clinical standards of dose calculation in brachytherapy have been based on the TG-43 report issued in 1995 by the American Association of Physicists in Medicine (AAPM) [1, 2]. This report considers all tissues in the CT as water, including applicators or shielding. This approximation may have minor consequences for high energy brachytherapy sources, such as the ¹⁹²Ir, where photons interact mainly via Compton scattering. However, for lower energy sources such as the ¹⁰³Pd or the ¹²⁵I, photoelectric effect is one of the main interaction mechanisms, which has an interaction probability that depends strongly on the average atomic number (Z) of the tissue [3]. Consequently, in 2012 the TG-

186 guidelines [4] were published, indicating that the water-based TG-43 dosimetry should be replaced by model-based dose calculation algorithms (MBDCAs).

The INTRABEAM system (Carl Zeiss Surgical GmbH, Oberkochen, Germany) is a commercial device for low energy X-ray intraoperative radiation therapy (IORT), also called electronic brachytherapy. It is a mobile accelerator that includes a miniature electron-beam driven 50 kVp X-ray source [5, 6]. It is primarily used for partial breast irradiation treatments [7-9], which are performed with spherical applicators (of sizes from 1.5 to 5 cm diameter) attached to the X-ray source and inserted in the tumor cavity. This technique has showed some benefits in comparison to external beam radiotherapy, such as similar local control with less toxicity [8, 10]. Up to date there is only one commercial Treatment Planning System (TPS) for IORT. Radiance [11], developed by the GMV company (Tres Cantos, Spain), is a TPS for both electron and X-rays IORT, and in the case of INTRABEAM, it includes a Monte Carlo (MC) based dose computation algorithm [12, 13]. But in practice, the treatment planning with the INTRABEAM system is still done in most clinics by determining the treatment time based on tabulated values of depth dose rate in water for a calibrated source and the prescription dose at a depth of interest [14].

MBDCAs offer more accurate treatment plans [15], provided that a detailed knowledge of both the tissue composition and density derived from the planning images is available [16]. This is however challenging in the breast, as adipose and glandular tissue have similar Hounsfield Units (HU) and disentangling both is not always feasible [3]. Despite their similarities in HU, both tissues differ considerably in their effective atomic number, which results in different dose depositions under low-energy photons.

TG-186 also reports that, if a segmentation of the breast cannot be safely done, a single average tissue composition should be chosen instead [4]. However, breast tissue composition is very variable [17]. Probably due to this, different single tissues have been proposed in the literature. A 50% glandular – 50% adipose (by fraction of weight) average breast tissue has been extensively considered as a standard model in mammography [18]. However, Yaffe *et al* [19], after performing a study on 1340 women, concluded that the average breast tissue should be an 20% glandular – 80% adipose mix instead.

Several works have studied dose differences due to breast composition during low energy radiations, mostly for brachytherapy seeds, and found indeed a large effect [16, 20-25]. Afsharpour *et al*. [26] evaluated the dose sensitivity to tissue heterogeneities in breast for permanent ^{103}Pd seeds, and found differences in dose distributions computed from MBDCAs or TG-43 plans of up to 24%. White *et al*. [3] compared the dose estimated following TG-43 and TG-186 guidelines in breast for the Xofig Axxent electronic brachytherapy source and found differences in predicted dose to all volumes of interest. They also found that TG-43 overestimated the dose to certain regions in the body but underestimated in other regions such as the ribs. A review of previous studies regarding differences in dose between water-based and MBDCAs, including breast, was presented by Mann-Krzisnik *et al* [16].

Following TG-186 recommendations is always the most suitable option, as it provides the most accurate results. However, in the case of breast this is not always possible given the difficulty of extracting accurate soft tissue composition from CT data. Consequently, the aim of this work was to identify the single tissue in the breast that best reproduces the dose obtained following the TG-186 recommendations. To do this, we studied the effect on the estimations of dose deposited in the breast structures with the INTRABEAM device with different soft tissue assignment strategies, from the water-based TG-43 recommendation to the most realistic model-based TG-186, including in between 4 single composition-breast tissues with different adipose-glandular percentages. Breast CT images from five patients were used to perform the comparisons.

2. MATERIALS AND METHODS

2.1. Clinical cases

A treatment plan for a partial breast irradiation was made in five preoperative thorax CTs. The CT image data were anonymized. DICOM images were cropped into the area of interest and interpolated to have the same voxel size ($1 \times 1 \times 1 \text{ mm}^3$). Three Regions of Interest (ROIs) were selected in the CTs segmented with the reference tissue assignment strategy described in section 2.3: A ROI including only adipose tissue (in pink in Figure 1 (b)), a ROI with only glandular tissue (in red in Figure 1 (b)) and an *average* ROI including both adipose and glandular tissues (in yellow in Figure 1(b)). An example of the selected ROIs of one of the CTs studied is presented in Figure 1(b).

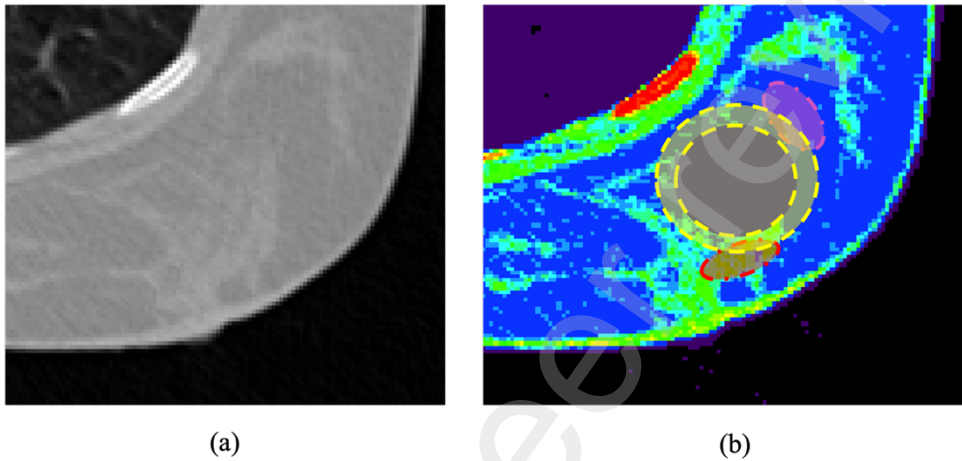


Figure 1. Original CT (a) and the segmented CT (b) from the conversion from HU to tissue, according to the reference tissue model of section 2.3. Looking inside the segmented breast in (b), adipose tissue appears in blue and glandular in green. The applicator is shown in grey, together with the three ROIs analyzed in the study: Adipose (pink), glandular (red) and average (yellow).

2.2. Monte Carlo simulation

PenEasy [27], a main program developed for PENELOPE-2008 [28], was used to perform the simulations. First, the X-ray source (XRS) of the INTRABEAM was simulated in detail to obtain the energy spectrum. Then, the energy spectrum was used to calculate a Phase-Space (PHSP) file of a 3 cm diameter spherical applicator. Finally, the PHSP file was placed in the patient's geometry and dose was computed.

a) Source description

The simulation of the XRS was defined according to the literature [5, 12, 14, 29-31]. It consisted of a 1.6 cm length beryllium needle with 1.1 mm inner radius and thickness of 0.5 mm with a $0.5 \mu\text{m}$ layer of gold at the end of the probe. It was surrounded by a first layer of nickel and a second layer of TiN. The electron beam impacted on an annular area between 0.6 and 0.8 mm radii [29] and had a Gaussian energy distribution with a mean energy of 50 keV and a full width at half maximum (FWHM) of 5 keV. The energy spectrum was scored from $5 \cdot 10^{10}$ initial particles at the exit of the probe surface.

b) Phase Space of the spherical applicator

The energy spectrum from the needle was used to generate a PHSP of a 3 cm diameter spherical applicator [12]. A quasi-punctual source of photons emitting isotropically from the center of the applicator was simulated, and a PHSP with 10^{10} particles was stored outside the applicator.

c) Patient simulation

Finally, the PHSP file from the 3 cm diameter spherical applicator was placed in the geometries of the

converted CTs with the different tissue assignments and dose was computed with 10^{10} initial particles. The energy cutoff of the photons was set to 1 keV and voxel size was $1 \times 1 \times 1 \text{ mm}^3$.

2.3. Reference dose distributions

An accurate segmentation of the CTs was used to calculate the reference dose distributions following the TG-186 recommendations [4]. The identification of tissue materials and densities from the CTs was done following Schneider *et al.* [32]. They made a correlation between the HU from 71 human tissues and the tissue parameters and obtained functions to convert the HU into the mass density and the elemental weights in the skeletal and soft tissue HU ranges. The skeletal functions were generated considering a mix of osseous tissue and bone marrow, and for the soft tissue, a mix of fat and water was considered. This way, one can generate as many artificial but biological tissues as needed whose elemental composition and density will correlate with the CT numbers. In this work, we used the same parameterization of the scale of HU as Schneider *et al.* and we segmented the scale into 24 biological materials. Densities were calculated from formulas (19), (21) and (23) in said reference. The elemental composition of the 24 biological materials is presented in Table 1.

Table 1. Table extracted from [32] with the elemental composition of the 24 biological materials used for the segmentation of the reference model.

| HU | Elemental weights (%) | | | | | | | | | | | |
|--------------|-----------------------|------|------|------|-----|-----|------|-----|-----|-----|-----|------|
| | H | C | N | O | Na | Mg | P | S | Cl | Ar | K | Ca |
| -1000 – -950 | | | 75.5 | 23.2 | | | | | | 1.3 | | |
| -950 – -120 | 10.3 | 10.5 | 3.1 | 74.9 | 0.2 | | 0.2 | 0.3 | 0.3 | | 0.2 | |
| -120 – -83 | 11.6 | 68.1 | 0.2 | 19.8 | 0.1 | | | 0.1 | 0.1 | | | |
| -82 – -53 | 11.3 | 56.7 | 0.9 | 30.8 | 0.1 | | | 0.1 | 0.1 | | | |
| -52 – -23 | 11.0 | 45.8 | 1.5 | 41.1 | 0.1 | | 0.1 | 0.2 | 0.2 | | | |
| -22 – 7 | 10.8 | 35.6 | 2.2 | 50.9 | | | 0.1 | 0.2 | 0.2 | | | |
| 8 – 18 | 10.6 | 28.4 | 2.6 | 57.8 | | | 0.1 | 0.2 | 0.2 | | 0.1 | |
| 19-80 | 10.3 | 13.4 | 3.0 | 72.3 | 0.2 | | 0.2 | 0.2 | 0.2 | | 0.2 | |
| 81-120 | 9.4 | 20.7 | 6.2 | 62.2 | 0.6 | | | 0.6 | 0.3 | | | |
| 121-200 | 9.5 | 45.5 | 2.5 | 35.5 | 0.1 | | 2.1 | 0.1 | 0.1 | | 0.1 | 4.5 |
| 201-300 | 8.9 | 42.3 | 2.7 | 36.3 | 0.1 | | 3.0 | 0.1 | 0.1 | | 0.1 | 6.4 |
| 301-400 | 8.2 | 39.1 | 2.9 | 37.2 | 0.1 | | 3.9 | 0.1 | 0.1 | | 0.1 | 8.3 |
| 401-500 | 7.6 | 36.1 | 3.0 | 38.0 | 0.1 | 0.1 | 4.7 | 0.2 | 0.1 | | | 10.1 |
| 501-600 | 7.1 | 33.5 | 3.2 | 38.7 | 0.1 | 0.1 | 5.4 | 0.2 | | | | 11.7 |
| 601-700 | 6.6 | 31.0 | 3.3 | 39.4 | 0.1 | 0.1 | 6.1 | 0.2 | | | | 13.2 |
| 701-800 | 6.1 | 28.7 | 3.5 | 40.0 | 0.1 | 0.1 | 6.7 | 0.2 | | | | 14.6 |
| 801-900 | 5.6 | 26.5 | 3.6 | 40.5 | 0.1 | 0.2 | 7.3 | 0.3 | | | | 15.9 |
| 901-1000 | 5.2 | 24.6 | 3.7 | 41.1 | 0.1 | 0.2 | 7.8 | 0.3 | | | | 17.0 |
| 1001-1100 | 4.9 | 22.7 | 3.8 | 41.6 | 0.1 | 0.2 | 8.3 | 0.3 | | | | 18.1 |
| 1101-1200 | 4.5 | 21.0 | 3.9 | 42.0 | 0.1 | 0.2 | 8.8 | 0.3 | | | | 19.2 |
| 1201-1300 | 4.2 | 19.4 | 4.0 | 42.5 | 0.1 | 0.2 | 9.2 | 0.3 | | | | 20.1 |
| 1301-1400 | 3.9 | 17.9 | 4.1 | 42.9 | 0.1 | 0.2 | 9.6 | 0.3 | | | | 21.0 |
| 1401-1500 | 3.6 | 16.5 | 4.2 | 43.2 | 0.1 | 0.2 | 10.0 | 0.3 | | | | 21.9 |
| 1501-1600 | 3.4 | 15.5 | 4.2 | 43.5 | 0.1 | 0.2 | 10.3 | 0.3 | | | | 22.5 |

2.4. Tissue assignment strategies

Six Tissue Assignment Strategies (TASs) were defined to study the effect of the tissue composition on the dose distributions. The elemental composition of the glandular and adipose tissues were defined following the ICRU report #46 [33]. The averaged breast tissues in this work were specified as percent mixtures by mass. The whole geometry contained a single average tissue, including ribs, lung, skin and air. The elemental composition of the different tissues can be seen in Table 2. The TASs were defined as follows:

1. *TG-43*: All voxels were assigned as water with unity density.
2. *Water*: All voxels were assigned as water with CT-derived densities.

3. *Adipose*: All voxels were assigned as adipose tissue with CT-derived densities.
4. *Glandular*: All voxels were assigned as glandular tissue with CT-derived densities.
5. *Breast-5050*: All voxels were assigned as an average breast tissue 50% adipose - 50% glandular (by fraction of weight) with CT-derived densities.
6. *Breast-8020*: All voxels were assigned as an average breast tissue 80% adipose – 20% glandular (by fraction of weight) with CT-derived densities.

Table 2. Elemental compositions according to the ICRU 46 report for the tissue assignments

| Tissue | Elemental weights (%) | | | | | | | |
|-------------|-----------------------|------|------|------|-----|------|------|-----|
| | H | C | N | O | Na | P | S | Cl |
| Glandular | 10.6 | 33.2 | 3.0 | 52.7 | 0.1 | 0.1 | 0.2 | 0.1 |
| Adipose | 11.4 | 59.8 | 0.7 | 27.8 | 0.1 | | 0.1 | 0.1 |
| Breast-5050 | 11.0 | 46.5 | 1.9 | 40.3 | 0.1 | 0.1 | 0.2 | 0.1 |
| Breast-8020 | 11.3 | 54.8 | 1.13 | 32.5 | 0.1 | 0.02 | 0.12 | 0.1 |

2.5. Evaluation of tissue assignment strategies

The average dose in the ROIs previously defined in the CTs of all TASs were compared to the reference by means of relative differences, defined as:

$$diff(\%) = \frac{\overline{dose_{REF}} - \overline{dose_{TAS}}}{\overline{dose_{REF}}} 100 \quad (1)$$

Where $\overline{dose_{REF}}$ is the average dose in the ROI from the reference and $\overline{dose_{TAS}}$ is the average dose in the ROI of the evaluated strategy. Positive values mean lower dose than the reference, which imply an *over-prescription of the dose*. Negative values mean a higher dose in the ROI than the reference, which lead to an *under-prescription of the dose*.

In addition to the relative differences, dose ratio maps comparing dose distributions were generated. The ratios were done with a voxel-by-voxel comparison between the reference and the evaluated strategy.

3. RESULTS

3.1. Dose profiles and dose ratios in the breast

Figure 2a presents a 2-Dimensional (2D) reference dose distribution obtained from one accurately segmented CT and Figure 2b shows dose profiles along the yellow line on the 2D dose map, obtained with different TASs. For tissues outside the breast, no TAS was able to adequately reproduce the reference dose. This was expected as these tissues (lung, bone, muscle, skin) were not included in the assignment strategies considered. Inside the breast, the reference profile was quite irregular, following the detailed segmentation, with relatively larger doses in glandular tissue and smaller in adipose (see red arrows in Figure 2b marking the transition between dose absorbed in glandular and adipose regions). Along regions where glandular tissue dominates, dose profiles obtained from *TG-43*, *water* and *glandular* TASs were very similar to the reference dose. In adipose regions, where the reference dose is smaller, the reference dose profile comes closer to the dose profiles obtained using *adipose* or *breast-8020* TASs.

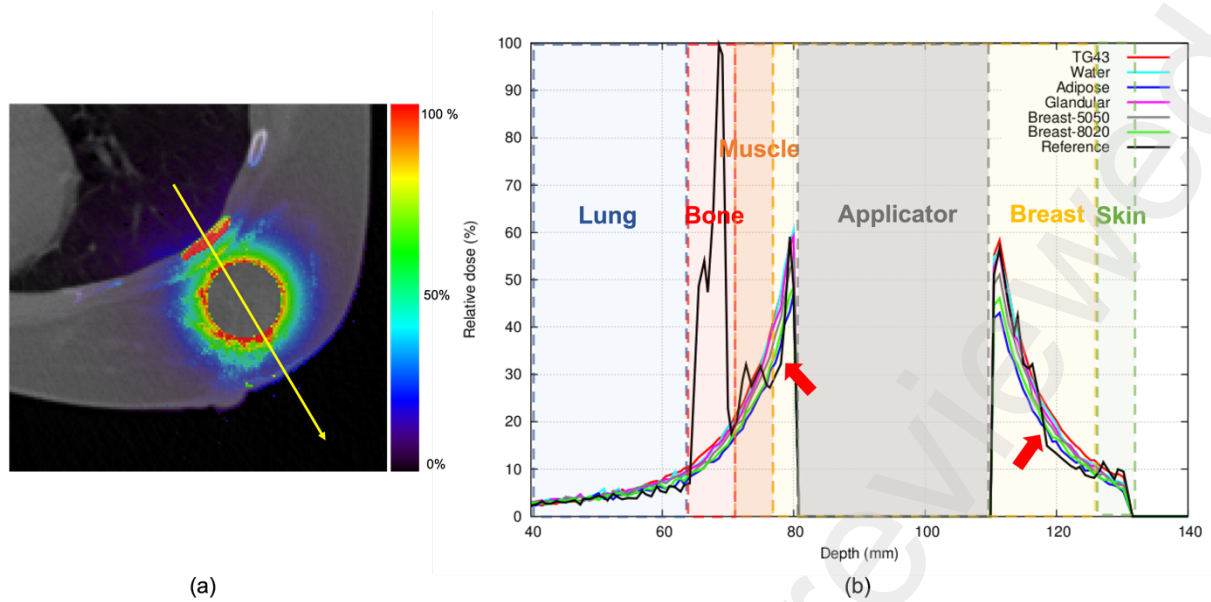


Figure 2. (a) 2D reference dose distribution in a patient's CT, and the dose profiles (b) from different TASs along the yellow arrow in (a). The red arrows point to the regions where transition between glandular and adipose tissues occurs.

This behavior can be better appreciated in Figure 3, where dose ratios between reference and the TASs are presented for a 2D slice of the CT of one of the patients. In this figure, one can see how dose in adipose tissue was overestimated by up to a 30% in dose calculations based upon the different TASs, except in the *adipose* TAS, where dose was accurately reproduced, and in the *breast-8020* TAS, where the overestimation was only 10%. In glandular tissue, *TG43*, *water* and *glandular* TASs reasonably reproduced the dose while the other assignment strategies underestimated the dose in this tissue by 10% to 30%. Notice how all strategies underestimated the dose in the skin and in the muscle up to 30-40% and in the bone by more than 50%.

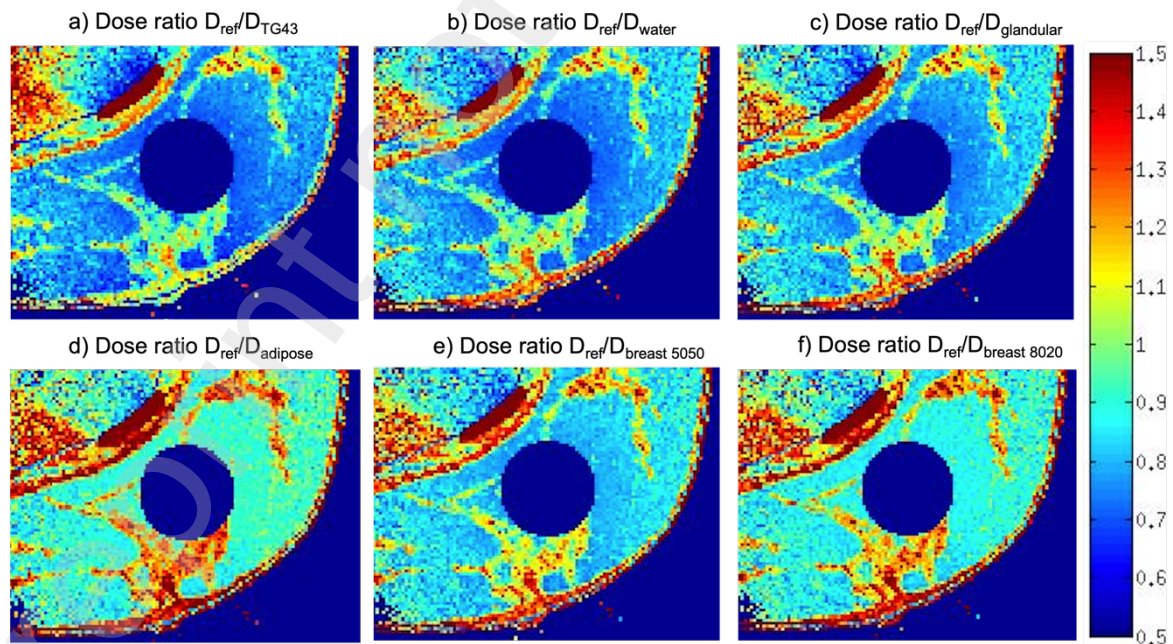


Figure 3. Dose ratio maps for one of the patients between the dose computed with the fully segmented reference model against the dose computed from different TASs. The dose inside the applicator and outside the patient is disregarded and appears in dark blue.

3.2. Relative differences in the regions of interest

Figure 4 shows a box plot with the relative differences found in all the ROIs for the five patients evaluated. Keep in mind that positive values refer to lower doses than the reference, which translates into over-prescription of dose, while negative values refer to higher doses than the reference, which means dose under-prescription.

Again, one can see that the *glandular* and *adipose* TASs reproduced accurately dose distributions in their corresponding tissues within the breast. The dose in the adipose ROI was also reasonably reproduced with the *breast-8020* TAS, with a relative difference below 5% in all cases. The other TASs overestimated the dose in the adipose ROI, which led to under-prescription of more than 10% with *breast-5050* TAS and more than 30% with the *TG-43* TAS. As we have shown before, the dose in the glandular ROI was reasonably estimated also by *TG-43* and *water* TASs. The other assignment strategies underestimated the dose in this ROI, leading to an over-prescription of around 5% with *breast-5050* TAS, about 10-15% with *breast-8020* TAS, and more than 15% with the *adipose* TAS. Finally, if we study the dose in the average (glandular + adipose) ROI, we can see that the best results were obtained with *adipose* and *breast-8020* TASs. The first one slightly over-prescribed the dose by less than 7% (4% overall), and the second one slightly under-prescribed the dose by less than 6% (3% overall). The other strategies overestimated the dose, being *TG-43* TAS the least accurate one, leading to dose under-prescription by up to 30% in the worst case.

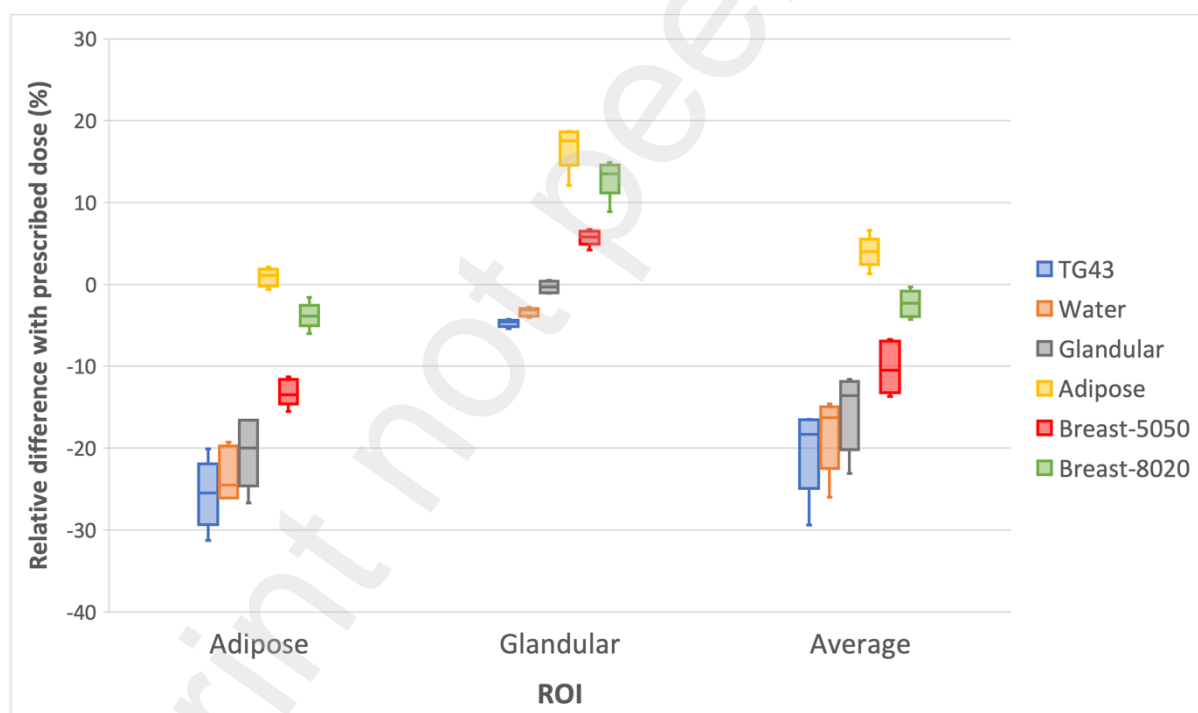


Figure 4. Box plot with the relative dose differences between each TAS and the reference measured in the selected ROIs for the five patients evaluated.

4. DISCUSSION AND CONCLUSION

The effect of the breast tissue composition on the dose for low energy photons has been extensively studied in the literature, mainly for low-energy brachytherapy. In this work we have extended the study to the INTRABEAM, because despite being a commonly used device for performing IORT in breast, most planning with the INTRABEAM is still being done based on TG-43 dose distributions.

To study this effect, we compared dose obtained from fully segmented CTs with doses obtained from six tissue assignment strategies. When we selected a ROI in the breast that included both glandular and adipose tissues (an “average” breast ROI), we saw that considering the breast made only of adipose tissue with CT-derived densities gave reasonable results, underestimating the dose only by a few percent, which would lead to an over-prescription of the dose of less than 7%. Replacing the soft tissues within the breast by a single tissue made of 80% adipose and 20% glandular tissues, with CT-derived densities, provided also reasonable results, although it produced a slightly under-prescription of the dose (less than 6% in the worst case) in the average soft tissue. In contrast, considering the breast as a single tissue made of 50% adipose and 50% glandular, with CT-derived densities, was proven insufficient to reproduce the reference dose in the 5 cases evaluated, overestimating dose in the average ROI in all cases by up to a 15%. Similar results were found when we considered the breast as 100% glandular with CT-derived densities, where dose was overestimated by more than 20%.

Finally, the worst predictions were obtained when dose was planned in water, as it overestimated the prescribed dose, and thus treatment plans yielded a dose up to 30% lower than intended. This was quite independent on whether we assigned unity density or derived density from HU to all tissues in breast, as this did not significantly alter the dose distribution. This result agrees with Afsharpour *et al.* [26], that showed that the effect of the elementary composition outweighs the effect of the density on dose distributions.

Previous works showed similar results for other low-energy devices. These results included, for example, differences up to 25% when comparing a model-based simulation with a water-based using a ^{103}Pd brachytherapy source [24, 26] and differences up to 40% with the Xofigo Axxent electronic brachytherapy source [3, 4]. These results are in line with the 20%-30% differences we obtained when comparing the water-based dose distributions to the references.

INTRABEAM is becoming increasingly used for breast irradiations, but some decisions regarding the treatment such as the irradiation time are still based on dose in water. In this work we showed that dose planning in water leads to an under-prescription of the dose by more than 30%. Therefore, the sensitivity of the tissues to the INTRABEAM working energies needs to be revised. Of course, an accurate segmentation of the breast tissues, as recommended by the TG-186 guidelines, should be the most desirable option. However, this is not always possible with single-energy CTs. In this case, that is, if correct soft tissue segmentation in the breast cannot be safely done, we believe that either a single tissue containing a mix of 80% adipose and 20% glandular, or even a 100% adipose single tissue, should be selected as the average soft tissue composition in breast for low-energy X-rays. An alternative could be the use of dual-energy CTs (DECT) or even spectral CTs, as their availability is increasing, especially with the escalation of proton therapy facilities. By combining information from multiple X-ray energies, soft tissue identification is largely simplified [16, 34, 35], allowing to identify different soft tissues of the breast accurately, and to increase the reliability of INTRABEAM plans.

Acknowledgments

This work was funded by Comunidad de Madrid under project B2017/BMD-3888 PRONTO-CM “Protontherapy and nuclear techniques for oncology”. Support by the Spanish Government (RTI 2018-098868-B-I00, RTC-2015-3772-1, XPHASE-LASER, CPP2021-008751 NEWMBI) as well as European Regional and Resilience Funds, and the European Union’s Horizon 2020 research and innovation program under the Marie Skłodowska-Curie grant agreement No 793576 (CAPPERAM) is acknowledged.

This is a contribution for the Moncloa Campus of International Excellence, “Grupo de Física Nuclear-UCM”, Ref. 910059. Part of the calculations of this work were performed in the “Clúster de Cálculo para Técnicas Físicas”, funded in part by UCM and in part by EU Regional Funds.

BIBLIOGRAPHY

- 1 Nath, R., et al.: 'Dosimetry of interstitial brachytherapy sources: recommendations of the AAPM Radiation Therapy Committee Task Group No. 43', *Med Phys*, 1995, 22, (2), 209-234. <https://doi.org/10.1118/1.597458>
- 2 Rivard, M.J., et al.: 'Update of AAPM Task Group No. 43 Report: A revised AAPM protocol for brachytherapy dose calculations', *Med Phys*, 2004, 31, (3), 633-674. <https://doi.org/10.1118/1.1646040>
- 3 White, S.A., et al.: 'Comparison of TG-43 and TG-186 in breast irradiation using a low energy electronic brachytherapy source', *Med. Phys*, 2014, 41 (6), 061701. <https://doi.org/10.1118/1.4873319>
- 4 Beaulieu, L., et al. : 'Report of the Task Group 186 on model-based dose calculation methods in brachytherapy beyond the TG-43 formalism: current status and recommendations for clinical implementation', *Med. Phys.* , 2012, 39, (10), 6208-6236. <https://doi.org/10.1118/1.4747264>
- 5 Dinsmore, M., et al. : 'A new miniature x-ray source for interstitial radiosurgery: Device description', *Med. Phys.*, 1996, 23, (1), 45-52. <https://doi.org/10.1118/1.597790>
- 6 Beatty, J., et al. : 'A new miniature x-ray device for interstitial radiosurgery: dosimetry', *Med. Phys.*, 1996, 23, (1), 53-62. <https://doi.org/10.1118/1.597791>
- 7 Kraus-Tiefenbacher, U., et al. : 'Intraoperative radiotherapy (IORT) for breast cancer using the intrabeam™ system', *Tumori*, 2005, 91, (4), 339-345. <https://doi.org/10.1177/030089160509100411>
- 8 Vaidya, J.S., et al. : 'Targeted intraoperative radiotherapy versus whole breast radiotherapy for breast cancer (TARGIT-A trial): an international, prospective, randomised, non-inferiority phase 3 trial', *The Lancet*, 2010, 376, (9735), pp. 91-102. [https://doi.org/10.1016/S0140-6736\(10\)60837-9](https://doi.org/10.1016/S0140-6736(10)60837-9)
- 9 Eaton, D.: 'Electronic brachytherapy—current status and future directions', *Brit. J. Radiol*, 2015, 88, (1049), 20150002. <https://doi.org/10.1259/bjr.20150002>
- 10 Veronesi, U., et al.: 'Intraoperative radiotherapy versus external radiotherapy for early breast cancer (ELIOT): a randomised controlled equivalence trial', *Lancet Oncol*, 2013, 14, (13), 1269-1277. [https://doi.org/10.1016/S1470-2045\(13\)70497-2](https://doi.org/10.1016/S1470-2045(13)70497-2)
- 11 Valdivieso-Casique, M., et al.: 'RADIANCE-A planning software for intra-operative radiation therapy', *Transl Cancer Res* 2015;4(2):196-209. doi: 10.3978/j.issn.2218-676X.2015.04.05
- 12 Vidal, M., et al. : 'Fast optimized Monte Carlo phase-space generation and dose prediction for low energy x-ray intra-operative radiation therapy', *Phys. Med. Biol.*, 2019, 64, (7), 075002. <https://doi.org/10.1088/1361-6560/ab03e7>
- 13 Ibáñez, P., et al. : 'XIORT-MC: A real-time MC-based dose computation tool for low-energy X-rays intraoperative radiation therapy', *Med. Phys.*, 2021, 48, (12), 8089-8106. <https://doi.org/10.1002/mp.15291>
- 14 Alvarez, D.S.A., et al.: 'Monte Carlo calculation of the relative TG-43 dosimetry parameters for the INTRABEAM electronic brachytherapy source', *Phys. Med. Biol.*, 2020, 65, (24), 245041. <https://doi.org/10.1088/1361-6560/abc6f1>
- 15 Rivard, M.J., et al. : 'Enhancements to commissioning techniques and quality assurance of brachytherapy treatment planning systems that use model-based dose calculation algorithms a', *Med. Phys*, 2010, 37, (6), 2645-2658. <https://doi.org/10.1118/1.3429131>
- 16 Mann-Krzisnik, D., et al. : 'The influence of tissue composition uncertainty on dose distributions in brachytherapy', *Radiother. Oncol.*, 2018, 126, (3), 394-410. <https://doi.org/10.1016/j.radonc.2018.01.007>
- 17 Landry, G., et al.: 'Sensitivity of low energy brachytherapy Monte Carlo dose calculations to uncertainties in human tissue composition', *Med. Phys.*, 2010, 37, (10), 5188-5198. <https://doi.org/10.1118/1.3477161>
- 18 <https://www.fda.gov/radiation-emitting-products/regulations-mqsa/mammography-quality-standards-act-regulations>, accessed October 2022
- 19 Yaffe, M., et al.: 'The myth of the 50-50 breast', *Med. Phys.*, 2009, 36, (12), 5437-5443. <https://doi.org/10.1118/1.3250863>
- 20 Enger, S.A., et al.: 'Model-based dose calculation algorithms for brachytherapy dosimetry', *Semin Radiat Oncol*, 2019, 30:77–86. <https://doi.org/10.1016/j.semradonc.2019.08.006>
- 21 Yousif, Y.A., et al.: 'A review of dosimetric impact of implementation of model-based dose calculation algorithms (MBDCAs) for HDR brachytherapy', *Phys. Eng. Sci. Med.*, 2021, 44, (3), 871-886. <https://doi.org/10.1007/s13246-021-01029-8>
- 22 Furstoss, C., et al.: 'Monte Carlo study of LDR seed dosimetry with an application in a clinical brachytherapy breast implant', *Med. Phys.*, 2009, 36, (5), 1848-1858. <https://doi.org/10.1118/1.3116777>
- 23 Afsharpour, H., et al.: 'Influence of breast composition and interseed attenuation in dose calculations for post-implant assessment of permanent breast 103Pd seed implant', *Phys. Med. Biol.*, 2010, 55, (16), 4547. <https://doi.org/10.1088/0031-9155/55/16/S09>
- 24 Miksys, N., et al.: 'Patient-specific Monte Carlo dose calculations for 103Pd breast brachytherapy', *Phys. Med. Biol.*, 2016, 61, (7), 2705. <https://doi.org/10.1088/0031-9155/61/7/2705>
- 25 Shamsabadi, R., et al.: 'Influence of breast tissue composition on dosimetric characteristics of therapeutic low energy X-rays', *Radiat. Phys. Chem.*, 2020, 177, 109110. <https://doi.org/10.1016/j.radphyschem.2020.109110>

- 26 Afsharpour, H., et al.: 'Tissue modeling schemes in low energy breast brachytherapy', *Phys. Med. Biol.*, 2011, 56, (22), 7045. <https://doi.org/10.1088/0031-9155/56/22/004>
- 27 Sempau, J., Badal, A., and Brualla, L.: 'A PENELOPE-based system for the automated Monte Carlo simulation of clinaes and voxelized geometries—application to far-from-axis fields', *Med. Phys.*, 2011, 38, (11), 5887-5895. <https://doi.org/10.1118/1.364302>
- 28 Salvat, F., et al. 'PENELOPE-2008: A code system for Monte Carlo simulation of electron and photon transport', OECD 2009, NEA No. 6416. <https://www.oecd-nea.org/upload/docs/application/pdf/2019-12/nea6416-penelope.pdf>
- 29 Clausen, S., et al. : 'A Monte Carlo based source model for dose calculation of endovaginal TARGIT brachytherapy with INTRABEAM and a cylindrical applicator', *Z Med Phys*, 2012, 22, (3), 197-204. <https://doi.org/10.1016/j.zemedi.2012.06.003>
- 30 Nwankwo, O., et al.: 'A virtual source model of a kilo-voltage radiotherapy device', *Phys. Med. Biol.*, 2013, 58, (7), 2363. <https://doi.org/10.1088/0031-9155/58/7/2363>
- 31 Yanch, J., and Harte, K.: 'Monte Carlo simulation of a miniature, radiosurgery x-ray tube using the ITS 3.0 coupled electron-photon transport code', *Med. Phys.*, 1996, 23, (9), 1551-1558. <https://doi.org/10.1118/1.597885>
- 32 Schneider, W., et al. : 'Correlation between CT numbers and tissue parameters needed for Monte Carlo simulations of clinical dose distributions', *Phys. Med. Biol.*, 2000, 45, (2), 459. <https://doi.org/10.1088/0031-9155/45/2/314>
- 33 'Photon, electron, proton and neutron interaction data for body tissues,' ICRU Report 46. International Commission on Radiation Units and Measurements, Bethesda, 1992. ISSN 0161-5505
- 34 Bazalova, M., et al.: 'Dual-energy CT-based material extraction for tissue segmentation in Monte Carlo dose calculations', *Phys. Med. Biol.*, 2008, 53, (9), 2439. <https://doi.org/10.1088/0031-9155/53/9/015>
- 35 Van Elmpt, W., et al.: 'Dual energy CT in radiotherapy: current applications and future outlook', *Radiother. Oncol.*, 2016, 119, (1), 137-144. <https://doi.org/10.1016/j.radonc.2016.02.026>